

Experimental Evaluation of Multiantenna Spectrum Sensing Detectors using a Cognitive Radio Testbed

J. Manco-Vásquez, J. Gutiérrez Terán, J. Perez-Arriaga, J. Ibañez, I. Santamaria
 Dept. of Communications Engineering, University of Cantabria, Spain
 E-mail: {juliocesar, jesusgt, jperez, jesus, nacho}@gtas.dicom.unican.es

Abstract—Cognitive radio (CR) is a promising approach to improve the efficiency use of the wireless spectrum. One key element of this technology is spectrum sensing, which allows secondary users to detect the presence of licensed (primary) users. To this end, multiantenna spectrum sensing techniques have been proposed to detect the presence of a primary user based solely on the correlation structure of the signal received by a cognitive secondary receiver equipped with multiple antennas. Despite the numerous theoretical studies in the area of spectrum sensing, there exists a lack of experimental work evaluating the performance of these techniques in practice. In this paper, we test the performance of multiantenna Bayesian and generalized likelihood ratio test (GLRT) detectors on a cognitive radio platform. In comparison to one-shot GLRT detectors, the Bayesian detector is able to exploit past information from previous sensing periods, thus learning from the environment and improving its performance. Our cognitive platform is composed of Universal Software Radio Peripheral (USRP) nodes, that emulate the behavior of a single-antenna primary and a multiantenna cognitive receiver. Our measurements show that the Bayesian detector outperforms the GLRT detectors, in both stationary and non-stationary environments.

Index Terms—Cognitive Radio, Bayesian Detection, Multiantenna Spectrum Sensing, Cognitive Testbed, USRP.

I. INTRODUCTION

The availability of spectral resources is being limited by a growing demand of wireless services [1]. Cognitive radio (CR) systems have been proposed to alleviate this limitation by achieving a more efficient use of the spectrum. In this context, a reliable spectrum sensing stage plays an important role, since it allows sharing the spectrum between legacy or primary users (PU) and non-legacy or secondary users (SU). By detecting holes in the spectrum, these gaps are filled with transmissions from SU, thus improving the usage of the frequency bands while avoiding interferences to licensed users.

Regarding the detection problem, some well-known approaches have been extensively studied, such as the energy-based detector, matched-filter detectors or the use of pilots [2], [3]. However, these well-know schemes also have some disadvantages, such as the requirement of a precise receiver calibration (knowledge of the noise variance), or the requirement of perfect synchronization. Recently, detectors employing multiple antennas have received increased attention because they do not require prior knowledge about the PU modulation format or the noise power, and are able to work with asynchronously sampled signals [4], [5]. The vast majority of these approaches are one-shot detectors which are

based on the GLRT. As an alternative to the GLRT approach, Bayesian detectors that exploit prior information about the environment have also been studied in [6]–[8].

In most of these works, the performance evaluation of the proposed spectrum sensing strategies is carried out by means of computer simulations. Recently, some experimental evaluations of spectrum sensing algorithms have been described in the literature. For instance, in [9] an energy-based detector is evaluated in multiple bands by employing multiple antennas at the cognitive receiver, thus enhancing its performance by exploiting the spatial dimension. Also, in [10] a comparison performance was conducted between detection algorithms based on the eigenvalues of the received covariance matrix. Despite these few works, there still exist a need of experimental evaluations of spectrum sensing techniques in real scenarios using CR testbeds and platforms [11], [12].

In an attempt to fill this gap, in this paper we experimentally evaluate the performance of a Bayesian detector, recently proposed in [6], by means of experimental measurements on a low-cost hardware platform. More specifically, the platform is composed of USRP nodes using 5 GHz radios and allow us to emulate a scenario in which a single-antenna PU accesses the channel with a given probability of occupancy, and a secondary (cognitive) receiver, equipped with two antennas, senses the channel and performs Bayesian inference to learn the environment. The measurements were performed in an indoor scenario, for which long-coherence times are typically observed. To be able to assess the performance of the method in channels with higher mobility, we use a beamforming-based procedure at the PU to induce some pre-defined channel variability. Our experimental results confirm the advantages of the Bayesian approach with respect to GLRT-based detectors.

The rest of the paper is organized as follows: In Section II, we give an overview of the proposed Bayesian spectrum sensing algorithm to be evaluated in our cognitive platform. The implemented testbed and the measurement setup are described in Section III and IV, respectively. We present the experimental results in Section V and finally, the paper concludes with a discussion of the results in Section VI.

II. MULTIAN TENNA SPECTRUM SENSING

By employing multiple antennas at the cognitive receiver, it is possible to fully exploit both the spatial and temporal structure of the received signals, and detect the presence of a PU without any knowledge about its signalling scheme

or the noise variance [6]–[8]. In this work we consider a scenario with a single-antenna PU and a cognitive receiver that senses the wireless medium N times through L independent antennas. The received signal at the baseband is stacked in an observation matrix $\mathbf{X}_t = [\mathbf{x}_t[1], \dots, \mathbf{x}_t[N]]$, where $\mathbf{x}_t[n] \in \mathbb{C}^L$ denotes the snapshot acquired at the n -th time instant within the t -th sensing period or frame (see Fig. 1).

The spectrum sensing problem can be formulated as the following binary hypothesis test

$$\begin{aligned} \mathcal{H}_1 : \mathbf{x}_t[n] &= \mathbf{h}_t s_t[n] + \mathbf{v}_t[n], \\ \mathcal{H}_0 : \mathbf{x}_t[n] &= \mathbf{v}_t[n], \end{aligned} \quad (1)$$

where $\mathbf{x}_t[n]$ denotes the $L \times 1$ vector of the n -th sample of the receiver signal, $s_t[n] \in \mathbb{C}$ is the primary signal, $\mathbf{h}_t \in \mathbb{C}^{L \times 1}$ describes the (unknown) single-input multiple-output (SIMO) channel between the transmitter and the cognitive receiver, and $\mathbf{v}_t[n] \in \mathbb{C}^{L \times 1}$ is the additive white Gaussian noise. We assume that the vector-valued observations under each hypothesis follow complex Gaussian distributions

$$\begin{aligned} \mathcal{H}_1 : \mathbf{x}_t[n] &\sim \mathcal{CN}(\mathbf{0}, \mathbf{R}_t), \quad n = 0, \dots, N-1. \\ \mathcal{H}_0 : \mathbf{x}_t[n] &\sim \mathcal{CN}(\mathbf{0}, \mathbf{D}_t), \quad n = 0, \dots, N-1. \end{aligned} \quad (2)$$

where \mathbf{R}_t is an arbitrary positive definite covariance matrix and \mathbf{D}_t is a diagonal covariance matrix. The resulting hypothesis testing problem is in short a test on the structure of a covariance matrix under Gaussian data. This topic has been well researched in the statistics and signal processing literature.

Notice also that the likelihood under each hypothesis depends on unknown parameters and therefore the hypotheses are composite. The most typical approach to solve this kind of testing problems is the GLRT. When the noise is independent and identically distributed (iid) at each antenna, the GLRT is the well-known Sphericity test¹, which is given by

$$\mathcal{L}_{\text{spher}} = \frac{|\mathbf{S}_t|^{1/L}}{(1/L) \text{trace}(\mathbf{S}_t)} \quad (3)$$

where $|\cdot|$ and $\text{trace}(\cdot)$ refer to the determinant and trace of a matrix respectively, and $\mathbf{S}_t = \mathbf{X}_t \mathbf{X}_t^H / N$ is the sample covariance matrix.

The iid case assumes a perfectly calibrated multiantenna cognitive receiver, which is in general hard to achieve. A more general testing problem that can accommodate calibration uncertainties in the different antenna front-ends, considers a generic diagonal noise covariance matrix under \mathcal{H}_0 . The GLRT for this problem is the Hadamard ratio [14] and is given by

$$\mathcal{L}_{\text{Hadam}} = \frac{|\mathbf{S}_t|}{\prod_{i=1}^L [\mathbf{S}_t]_{ii}} \quad (4)$$

where $[\mathbf{S}_t]_{ii}$ refers to the (i, i) th element of the sample covariance matrix \mathbf{S}_t .

¹Actually, for rank-deficient covariance matrices the GLRT is, in general, more complicated, as it was shown in [5]. However, when $L = 2$ (which is the scenario considered in the experimental setup of this paper) the GLRT coincides with the Sphericity test [13].

A. Bayesian detector

The main goal of this paper is the practical evaluation in realistic environments of a multiantenna Bayesian detector for CR that has been recently proposed in [6]. In comparison to GLRT (one-shot) based approaches, the Bayesian detector exploits statistical information obtained from past sensing periods. In the following, we provide a short description of this technique; for a full treatment of this topic the reader is referred to [6].

In the proposed Bayesian framework, prior distributions are placed directly on the spatial covariance matrices under \mathcal{H}_0 and \mathcal{H}_1 , as well as on the probability of the channel occupancy.

The main idea of the proposed procedure is depicted in Fig. 1. At each sensing frame, the cognitive receiver updates the posterior distributions for \mathbf{R}_t and \mathbf{D}_t from the priors existing at t and the likelihood obtained from \mathbf{X}_t . Conjugate priors are chosen in order to obtain closed-form expressions for the posteriors as indicated in [6].

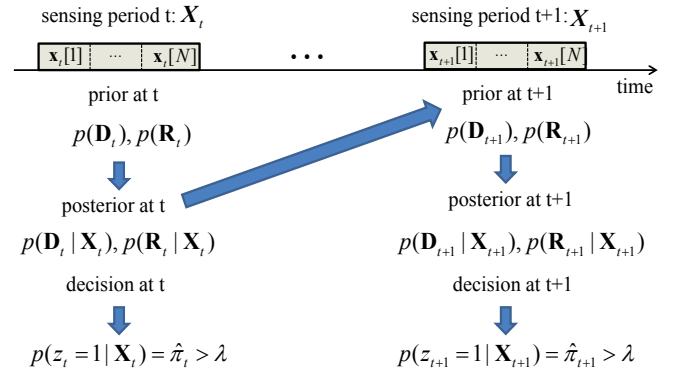


Fig. 1. A Bayesian framework for spectrum sensing: the posteriors obtained after processing a sensing frame are employed as priors for the next sensing frame.

The posterior of the channel occupancy $p(z_t = 1 | \mathbf{X}_t) = \hat{\pi}_t$ is then thresholded and used for detection, where the hidden variable z_t indicates whether the PU is active ($z_t = 1$) or not ($z_t = 0$). Specifically, as it was shown in [6], $\hat{\pi}_t$ can be obtained by blending the posterior and prior parameters according to

$$\hat{\pi}_t = \frac{1}{1 + \frac{|\check{\mathbf{D}}_t|^{\frac{\check{m}_t}{2}} |\check{\mathbf{R}}_t|^{\frac{\check{n}_t}{2}} \Gamma_L(\frac{\check{n}_t}{2}) \Gamma(\frac{\check{m}_t}{2})^L}{|\hat{\mathbf{R}}_t|^{\frac{\check{m}_t}{2}} |\hat{\mathbf{D}}_t|^{\frac{\check{n}_t}{2}} \Gamma_L(\frac{\check{n}_t}{2}) \Gamma(\frac{\check{m}_t}{2})^L}} \quad (5)$$

where $\Gamma_L(\cdot)$ and $\Gamma(\cdot)$ denote a multivariate gamma and a gamma function, respectively. Also, we have used $\check{\cdot}$ and $\hat{\cdot}$ to distinguish the prior and posterior parameters. The rest of the parameters are given by the following expressions:

$$\hat{n}_t = \check{n}_t + N \quad (6a)$$

$$\hat{\mathbf{R}}_t = \check{\mathbf{R}}_t + \mathbf{X}_t \mathbf{X}_t^H / N \quad (6b)$$

$$\hat{m}_t = \check{m}_t + N \quad (6c)$$

$$\hat{\mathbf{D}}_t = \check{\mathbf{D}}_t + \text{diag}(\mathbf{X}_t \mathbf{X}_t^H / N). \quad (6d)$$

where $\text{diag}(\cdot)$ refers to a matrix with their diagonal entries equal to the diagonal elements of the argument.

To handle non-stationary environments, a forgetting mechanism is introduced in the Bayesian detector. In particular, the prior parameters at the sensing frame $t + 1$ are a smoothed version of the posterior parameters at t and those used in the (uninformative) prior at $t = 0$

$$\check{n}_{t+1} = \lambda \hat{n}_t + (1 - \lambda) \check{n}_0 \quad (7a)$$

$$\check{\mathbf{R}}_{t+1} = \lambda \hat{\mathbf{R}}_t + (1 - \lambda) \check{\mathbf{R}}_0 \quad (7b)$$

$$\check{m}_{t+1} = \lambda \hat{m}_t + (1 - \lambda) \check{m}_0 \quad (7c)$$

$$\check{\mathbf{D}}_{t+1} = \lambda \hat{\mathbf{D}}_t + (1 - \lambda) \check{\mathbf{D}}_0, \quad (7d)$$

where $\lambda \in [0, 1]$ is a forgetting parameter. With this scheme, the cognitive receiver is able to both learn and forget information from past sensing frames, as needed. When $\lambda = 0$, all the information obtained from previous sensing frames is forgotten and the detector considers each frame independently (as the GLRT does). This would be adequate for very high-mobility scenarios and channels with high Doppler spreads. On the other hand, when $\lambda = 1$ no forgetting occurs and the posterior at t summarizes in an effective way all sensing data observed so far. This would be adequate in low-mobility scenarios.

III. TESTBED DESCRIPTION

For our cognitive radio platform, we have chosen USRP devices [15] developed by Ettus Research. The testbed also includes a universal hardware drive (UHD) as a host driver and a set of Application Programming Interface (API) functions. This UHD driver can be utilized as a standalone application or with third-party applications (e.g. Matlab). For the present work, we have developed our own application called Universal Software Architecture for Software Defined Radio (USASDR). This software architecture allows working simultaneously with several USRP nodes, by means of a unique controller identified by an IP address that receives instructions from a remote PC running Matlab.

The cognitive radio platform is composed of N210 USRP nodes. Each of them consists of a USRP motherboard and a Radio Frequency (RF) daughterboard. Basically, the motherboard consists of dual analog-to-digital converters (ADC) and digital-to-analog (DAC) converters connected to a Field Programmable Gain Array (FPGA). The FPGA downsamples the signal in the digital domain and transfers it to a Gigabit Ethernet controller. On the other hand, the daughterboard is a modular front-end used for analog operations such as up/down conversion.

The flow of signal in the receive path starts by down-converting the frequency of the received signal from RF to Intermediate Frequency (IF), around DC. Specifically, the XCVR2450 daughterboard based on a MAX2829 IC is able to cover industrial, scientific and medical (ISM) bands of 2.4GHz to 2.5GHz, and 4.9GHz to 5.8GHz. At this stage we obtain I/Q analog signals that are subsequently digitized by the ADC. The USRP motherboard contains 14-bit ADCs with



Fig. 2. N210 Ettus devices with the XCVR2450 daughterboard installed. A two-antenna cognitive receiver is composed of two N210 boards connected through a MIMO cable.

a sample rate of 100 MSamples/s. After sampling, the ADC transfers the data to an FPGA where data rate conversion is performed. Then, the FPGA transfers the results to Gigabit Ethernet controller which passes it over to the host computer where the rest of the signal processing tasks are performed.

Regarding the transmitter path, the same processing chain is repeated in reverse order. Firstly, the Gigabit Ethernet controller of the host computer sends the input data to the USRP. After receiving the complex signal, a digital up converter converts the signal to IF before passing it to a DAC with 16 bits of resolution and 400 MSamples/s of sample rate. The DAC finally sends the IF signal to the RF transceiver, where it is upconverted to RF and transmitted over the air.

In order to implement a multiantenna cognitive node, the N210 USRP node includes an specific expansion port that allows coherent synchronization of two USRP units, as it is depicted in Fig. 2. Since the same clock (oscillators) and time reference are shared, both USRP nodes can start transmitting/receiving at the same time, thus avoiding any synchronization problem.

IV. MEASUREMENT SETUP

We have considered a scenario where a single-antenna PU accesses the channel according to a predefined probability of occupancy and a cognitive receiver with two antennas senses the medium and performs the Bayesian detection procedure described in Section II-A. The experiments were conducted in the laboratory of the Signal Processing Group at the University of Cantabria, with a clear line of sight (LOS) between the PU and the cognitive receiver. When active, the PU transmits an orthogonal frequency division multiplexing (OFDM) 802.11a signal². Specifically, an OFDM waveform is generated with a rate of 9 Mbps using BPSK symbols, the resulting analog I/Q signals are sent to the RF front-end and transmitted at a carrier frequency of 5.6GHz. The power transmitted by the

²Remember, however, that the modulation format is assumed to be unknown and therefore is not exploited by the spectrum sensing techniques considered in this work.

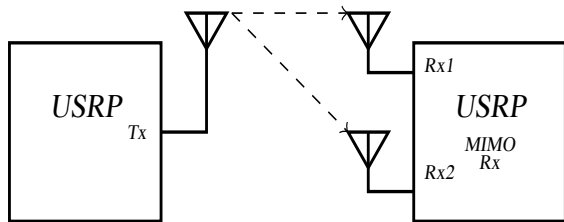


Fig. 3. Scheme of the proposed scenario: A single-antenna PU and a secondary user with two antennas.

PU can be modified, thus allowing us to control the received signal-to-noise ratio (SNR). We compare the performance of the proposed Bayesian detector, the Sphericity (iid case) and the Hadamard (non-iid) GLRT detectors.

A. Measurement Procedure

The PU starts transmitting according to a predefined periodic sequence of states \mathcal{H}_1 and \mathcal{H}_0 (See Fig. 4), which are obtained from the probability of channel occupancy that we have taken as 0.5. The PU stops transmitting after the secondary user (SU) has sensed the wireless channel and N samples have been acquired by the $L = 2$ antennas. The data acquired by the SU are transferred to the PC and the three detectors are tested. Then, a new transmitting/sensing cycle (either under \mathcal{H}_1 or \mathcal{H}_0) is performed as shown in Fig. 4.

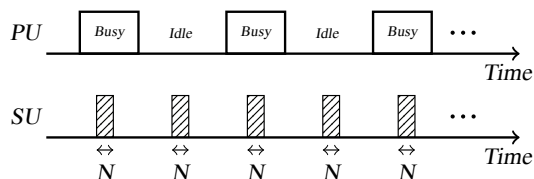


Fig. 4. A PU transmits according to a periodic sequence of states, and the SU senses the wireless channel in each state.

At each sensing period, the signals acquired by the two USRP nodes are used to estimate the sample covariance matrix. As it was described in Section II-A, the SU gathers statistical information summarized by the posterior densities on the covariance matrices. Therefore, we start computing the ROC curves after a given number of sensing frames has been sensed, so that the SU has obtained suitable prior information.

We carried out different measurement campaigns both in stationary and non-stationary environments. Typically, the indoor channel at 5 GHz under a controlled setup presents very long coherence times. In consequence, if no further action is taken the measurements are representative of a stationary environment. In order to test the performance under non-stationary environments, we should provide some mobility to either the PU or the SU. Since this mobility is very complicated to accomplish with our testbed, instead, we emulate a time-varying channel by transmitting the PU 802.11a signal using a time-varying beamformer. Basically, the idea consists on multiplying the PU OFDM signal by a 1×2 time-varying beamformer obtained according to an autoregressive model for

fading channel, thus providing correlated Rayleigh processes [16] as it is shown in Fig.5.

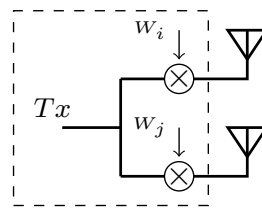


Fig. 5. Emulation of a time-varying channel by transmit beamforming.

V. EXPERIMENTAL RESULTS

We study the performance of the mentioned detectors by comparing their Receiving Operating Characteristic (ROC) curves obtained by measurements performed with our cognitive platform. For a given threshold we obtain the false alarm, P_{FA} , and detection probabilities, P_D , by averaging the results obtained over multiple transmitting/sensing cycles. We conducted experiments under static, slowly time-varying and fast time-varying environments. The mobility speed of the channel is controlled by the transmit beamforming procedure depicted in Fig.5. In a static scenario, we would expect to obtain covariance matrices (under each hypothesis) that remain almost constant over consecutive sensing periods, thus boosting the performance of the Bayesian detector in comparison to GLRT counterparts. The number of samples per each sensing frame was set to $N = 50$, and the forgetting factor λ was selected depending on the scenario mobility.

1) *Static scenario*: In Fig. 6 we compare the ROC obtained by the Bayesian detector using $\lambda = 1$ (curve marked with squares), the Sphericity (circles) and the Hadamard (crosses) detectors. For this example the SNR measured at the receiver was -7.3 dB. The improvement of the Bayesian detector over the GLRTs is evident. Notice, also, that the ROCs for the Sphericity and the Hadamard detectors are almost identical: this is due to the fact that in this example the noise variance in the two receiving branches is very similar.

2) *Slowly time-varying scenario*: In this scenario, we emulate a slowly time-varying channel by using the transmit beamforming procedure described previously. In this scenario, under a given hypothesis, the sample covariance matrix is correlated from frame to frame one as it is shown in Fig. 7. Nevertheless, the improvement of the Bayesian scheme is still evident.

3) *Fast time-varying scenario*: In our final experiment, we have studied the performance when the channel realizations in each sensing frame are iid (see Fig. 8). We note that our Bayesian detector still outperforms the other two detectors in this scenario. This can be explained to the fact that, under \mathcal{H}_0 , the diagonal covariance matrix remains constant and can be effectively learnt by the Bayesian detector.

VI. CONCLUSIONS

Using a cognitive radio testbed, in this paper we have evaluated the performance of three different multiantenna

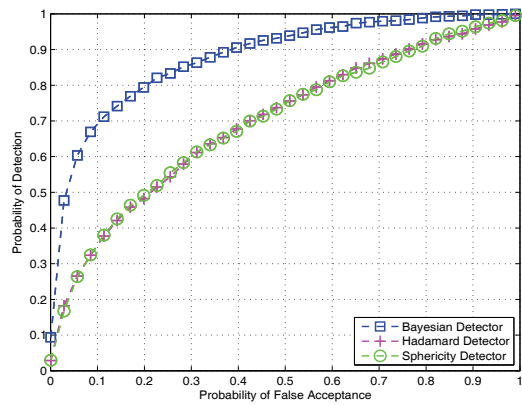


Fig. 6. ROC curves for the Bayesian (squares), Sphericity (circles) and Hadamard (crosses) detectors, in a static environment. $N = 50$ and a SNR = -7.3 dB was measured.

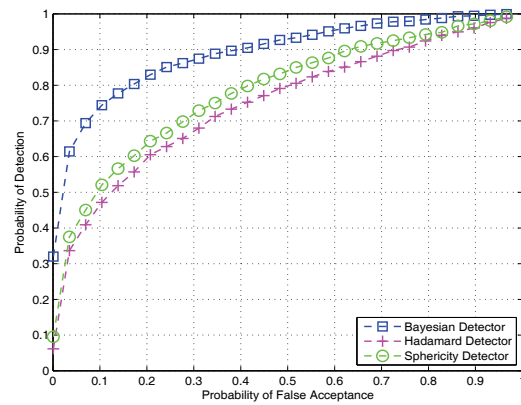


Fig. 8. ROC curves for the Bayesian (squares), Sphericity (circles) and Hadamard (crosses) detectors, in a fast time-varying environment. $N = 50$ and a SNR = -2.5 dB was measured.

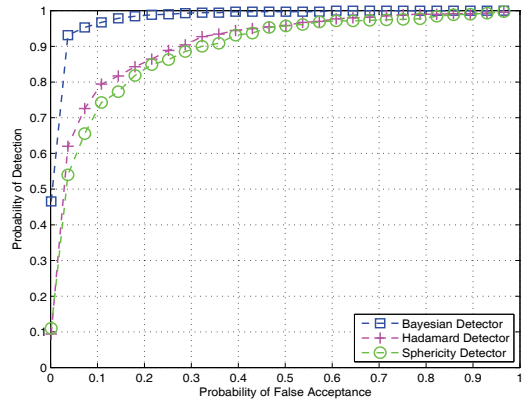


Fig. 7. ROC curves for the Bayesian (squares), Sphericity (circles) and Hadamard (crosses) detectors, in a slowly time-varying environment. $N = 50$ and a SNR = -1.18 dB was measured.

spectrum sensing algorithms in realistic static and time-varying environments. The experimental study shows that the Bayesian detector outperforms the GLRT detectors under the same conditions in different environments. A significant gain is obtained by the Bayesian detector since it exploits past information and is able to learn from the environment.

ACKNOWLEDGMENT

The research leading to these results has received funding from the Spanish Government (MICINN) under projects TEC2010-19545-C04-03 (COSIMA) and CONSOLIDER-INGENIO 2010 CSD2008-00010 (COMONSENS).

REFERENCES

[1] J. van de Beek, J. Riihijarvi, A. Achtzehn, and P. Mahonen, "TV white space in europe," *IEEE Transactions on Mobile Computing*, vol. 11, pp. 178–188, Feb. 2012.
 [2] T. Yucek and H. Arslan, "A survey of spectrum sensing algorithms for cognitive radio applications," *IEEE Communications Surveys & Tutorials*, vol. 11, no. 1, pp. 116–130, 2009.

[3] D. Cabric, A. Tkachenko, and R. Brodersen, "Spectrum sensing measurements of pilot, energy, and collaborative detection," in *Proc. of IEEE Military Communications Conference, 2006. MILCOM*, pp. 1–7, Oct. 2006.
 [4] P. Wang, J. Fang, N. Han, and H. Li, "Multiantenna-assisted spectrum sensing for cognitive radio," *IEEE Transactions on Vehicular Technology*, vol. 59, pp. 1791–1800, May. 2010.
 [5] D. Ramirez, G. Vazquez-Vilar, R. Lopez-Valcarce, J. Via, and I. Santamaria, "Detection of Rank-P signals in cognitive radio networks with uncalibrated multiple antennas," *IEEE Transactions on Signal Processing*, vol. 59, no. 8, pp. 3764–3774, 2011.
 [6] J. Manco-Vasquez, M. Lazaro-Gredilla, D. Ramirez, J. Via, and I. Santamaria, "Bayesian multiantenna sensing for cognitive radio," in *Proc. of IEEE Sensor Array and Multichannel Signal Processing Workshop (SAM)*, Jun 2012.
 [7] R. Couillet and M. Debbah, "A Bayesian framework for collaborative multi-source signal sensing," *IEEE Transactions on Signal Processing*, vol. 58, pp. 5186–5195, Oct. 2010.
 [8] J. Font-Segura and X. Wang, "GLRT-based spectrum sensing for cognitive radio with prior information," *IEEE Transactions on Communications*, vol. 58, no. 7, pp. 2137–2146, 2010.
 [9] M. Grimm, A. Krah, N. Murtaza, R. K. Sharma, M. Landmann, R. Thomä, A. Heuberger, and M. Hein, "Performance evaluation of directional spectrum sensing using an over-the-air testbed," in *Proc. of the 4th International Conference on Cognitive Radio and Advanced Spectrum Management*, pp. 17:1–17:5, ACM, Oct. 2011.
 [10] A. Mate, K.-H. Lee, and I.-T. Lu, "Spectrum sensing based on time covariance matrix using GNU radio and USRP for cognitive radio," in *Systems, Applications and Technology Conference (LISAT), 2011 IEEE Long Island*, pp. 1–6, may 2011.
 [11] D. Cabric and R. Brodersen, "Physical layer design issues unique to cognitive radio systems," vol. 2, pp. 759–763, Proc. of IEEE Personal, Indoor and Mobile Radio Communications, 2005. PIMRC 2005, Sept. 2005.
 [12] S. Mubaraq Mishra, D. Cabric, C. Chang, D. Willkomm, B. van Schewick, A. Wolisz, and R. W. Brodersen, "Implementation issues in spectrum sensing for cognitive radios," in *Proc. of IEEE Signals, Systems and Computers, 2004*, vol. 1, pp. 772–776, Nov. 2004.
 [13] J. W. Mauchly, "Significance test for sphericity of a normal n-variate distribution," *The Annals of Mathematical Statistics*, vol. 11, pp. 204–209, Jun. 1940.
 [14] S. S. Wilks, "On the independence of k sets of normally distributed statistical variables," *The Annals of Mathematical Statistics*, vol. 3, pp. 309–326, Jul. 1935.
 [15] "Ettus research LLC. Universal Software Radio,," Jun. 2012.
 [16] K. Baddour and N. Beaulieu, "Autoregressive modeling for fading channel simulation," *IEEE Transactions on Wireless Communications*, vol. 4, pp. 1650–1662, July 2005.